Electrochemical Capacitor Behavior of RuO_2 vertically Aligned Rods Filled with $RuO_2 \bullet xH_2O$

Diah Susanti, Dah-Shyang Tsai*, Chia-Liang Cheng, Department of Chemical Engineering, Ying-Sheng Huang, Alexandru Korotcov, Department of Electronic Engineering, National Taiwan University of Science and Technology (NTUST), Taipei 106 Taiwan

Introduction and Experimental details

A designed microstructure is proposed to fabricate high capacitance capacitors based on ruthenium dioxide. One dimensional RuO_2 rods (RuO_2NR) of high corrosion resistance and electrical conductivity acted as the electron conduits to collect and distribute charge. Meanwhile the hydrous RuO_2 ($RuO_2 \bullet xH_2O$) of high capacitance was coated on RuO_2NR to store charge. The capacitor of hybrid structure may possess the merits of hydrous and anhydrous RuO_2 both. In this work, we prepare a micron-meter thick hybrid electrode of anhydrous and hydrous RuO_2, and analyze its electrochemical capacitive behavior using cyclic voltammetry and impedance spectroscopy.

Anhydrous RuO_2 vertical rods were grown on $LiNbO_3(100)$ substrates via metalorganic CVD. The ruthenium source was a high-purity liquid precursor, bis(ethylcyclopentadienyl)Ru (Strem Chemicals). The substrate temperature was set at 340°C and the chamber pressure 2 Torr. Specimens of the RuO_2 rods on $LiNbO_3(100)$ substrates are denoted as RuO_2VR. The hybrid electrode which was prepared by electrodepositing hydrous RuO_2 on RuO_2VR is denoted as RuO_2VR-H. Capacitive properties were measured using two voltage modulation methods. In cyclic voltammetry (CV), the voltage modulation was done at various scan rates. In electrochemical impedance spectroscopy (EIS), the voltage modulation was to apply a sinusoidal alternating voltage of frequency $10^{-2} – 10^6$ Hz.

Results and Discussion

Morphological features of RuO_2VR and RuO_2VR-H are illustrated in Fig. 1. Typical vertical rods are 110-180 nm in diameter and 2600 nm in height in the RuO_2 one-dimensional assembly, as shown in Fig. 1(a). These densely-packed rods have a pyramidal tip and connected at the roots of the rods assembly. Considerable pore space is present among the rods can be filled with hydrous RuO_2. Hydrous RuO_2 of $RuO_2 \bullet 0.46H_2O$ is estimated to fill 80% of the pore space in RuO_2VR. The top and cross-sectional views of RuO_2VR-H are shown in Figs. 1(c) and 1(d). Fig. 1(b) is a schematic diagram indicating the RuO_2VR-H structure and the porous nature of $RuO_2 \bullet 0.46H_2O$.

Cyclic voltammograms of RuO_2VR at scan rate 5, 10, 25, 50, 100, 500 mVs^{-1} are plotted as accessible capacitance versus potential in the range of 0.0 - 1.0 V, Fig. 2(a). The CV capacitance of RuO_2VR decreases slightly with the increasing scan rate, from 25.8 $mFcm^{-2}$ (32.3 Fg^{-1}) at 25 mVs^{-1} to 22.3 $mFcm^{-2}$ (27.9 Fg^{-1}) at 1000 mVs^{-1}, indicating a weak dependence on the scan rate. The CV diagrams of RuO_2VR-H at various scan rates are illustrated in Fig. 2(b). In contrast to the low capacitance of RuO_2VR, the capacitance of RuO_2VR-H is much higher. The capacitance of

RuO$_2$VR-H is 464 mFcm^{-2} (403 Fg^{-1}) at 5 mVs^{-1}. But the capacitance value of RuO$_2$VR-H is influenced by the scan rate considerably. Fig. 2(b) indicates that the enclosed area of RuO$_2$VR-H decreases with the increasing scan rate. The specific capacitance of RuO$_2$VR-H drops 70% when the scan rate is raised to 1000 mVs^{-1}, that is, from 464 mFcm^{-2} at 5 mVs^{-1} to 137 mFcm^{-2} at 1000 mVs^{-1}. Apparently the proton storage capability of RuO$_2\bullet$0.46H$_2$O is not fully utilized at high scan rates, because of the fractal nature of hydrous RuO$_2$ and the distributed resistance and capacitance in the remaining pores.

Nyquist plots of RuO$_2$VR and RuO$_2$VR-H at various potentials are plotted in Figs. 3(a) and 3(b). When the potential $\geq$ 0.2 V, the impedance plots display one or two depressed semicircles at high frequencies and a nearly vertical line along the imaginary axis Z$''$ at low frequencies. These nearly vertical lines suggest the characteristics of an ideally polarizable electrode. When the potential $\leq$ 0.2 V, a deviation from the 90° slope indicates a nonideally polarizable behavior, especially for RuO$_2$VR at 0.0 V. The marked deviation from 90° at 0.0 V is in line with the strong scan rate dependence of cathodic current below 0.1 V, shown in Fig. 2(a).

Insets of Figs. 3(a) and 3(b) display more impedance details around the semicircles. A region of 45° slope in the medium frequency range can be found in the Nyquist plot of RuO$_2$VR-H, but not RuO$_2$VR. The 45° slope at medium frequencies is a characteristic of transmission line behavior, in contrast to a Warburg 45° phase angle plot which arises at low frequencies when a diffusion-controlled process is rate-determining. The transmission line behavior is attributed to the distributed resistances and capacitances in RuO$_2\bullet$0.46H$_2$O, which is the main structural difference between RuO$_2$VR-H and RuO$_2$VR.

Figs. 4(a) and 4(b) are the Bode plots showing the frequency dependence of |Z| and phase angle of RuO$_2$VR. The Bode plots of RuO$_2$VR-H are illustrated in Figs. 4(c) and 4(d). For the discussion purpose, it is convenient to divide the impedance behavior into the low, medium, and high frequency regions. The low frequency region is defined as the region where the |Z| plot shows a slope near -1 and the value of phase angle is between -90° and -45°. The low frequency range for RuO$_2$VR is $\leq$ 10 Hz. In contrast, the low frequency range of RuO$_2$VR-H is $\leq$ 0.4 Hz. The high frequency range is defined as the region where the magnitude of impedance |Z| is weakly dependent on the frequency and the phase angle is close to zero. The high frequency range for RuO$_2$VR is $\geq$ 10^3 Hz, and that for RuO$_2$VR-H is $\geq$ 200 Hz. Hence the medium frequency range is between 10^3 and 10 Hz for RuO$_2$VR, 200 and 0.4 Hz for RuO$_2$VR-H.

The |Z| value of RuO$_2$VR in the low frequency range (<1 Hz) is 6 or 8 times higher than that of RuO$_2$VR-H. Since impedance is a measure of the ability of a circuit to resist the electrical current, a lower |Z| value of RuO$_2$VR-H suggests the extra RuO$_2\bullet$0.46H$_2$O makes the hybrid electrode less resistive. The frequency where the phase angle equals to -45° may be regarded as the capacitor response frequency. The capacitor response frequency of RuO$_2$VR ranges from 7 to 20 Hz, which means a response time of 0.14 - 0.05 s. On the other hand, the capacitor response frequency of RuO$_2$VR-H ranges from 0.3 to 0.9 Hz, giving a response time of 3.3 – 1.1 s. The sluggish response of RuO$_2$VR-H is mainly caused by its larger capacitance. We also calculated the capacitances according to $C=(2\pi f Z'')^{-1}$, in which f is frequency in Hz and Z$''$ the imaginary part of

impedance in Ωcm^2. The RuO$_2$VR capacitances at 0.01 Hz are 14-26 mFcm^{-2}, those of RuO$_2$VR-H are 172-429 mFcm^{-2} depending on DC potentials. These capacitance values are generally in line with those values measured by CV.

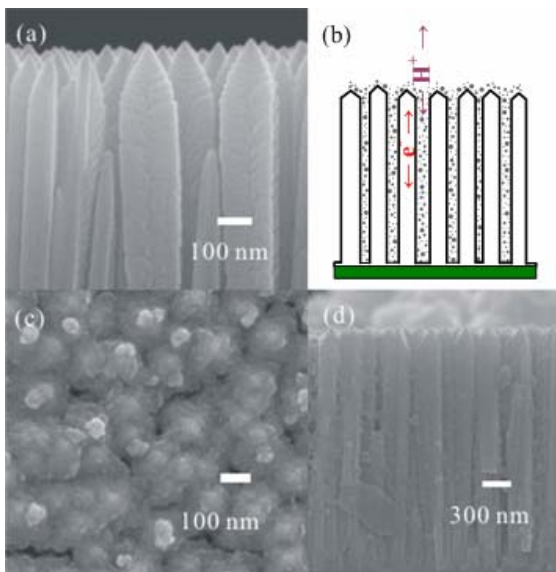Fig. 1 (a) The morphology of RuO$_2$VR, (b) a schematic diagram of RuO$_2$VR-H structure, (c) a top view of RuO$_2$VR-H showing the surface is covered by hydrous RuO$_2$, (d) a cross-sectional view of RuO$_2$VR-H.
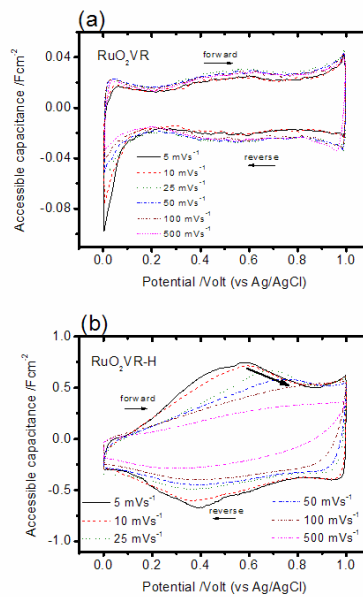

Fig. 2 CV diagrams of (a) RuO$_2$VR, (b) RuO$_2$VR-H at scan rate 5, 10, 25, 50, 100, 500 mVs^{-1}. Accessible capacitance is the ratio of response current divided by scan rate

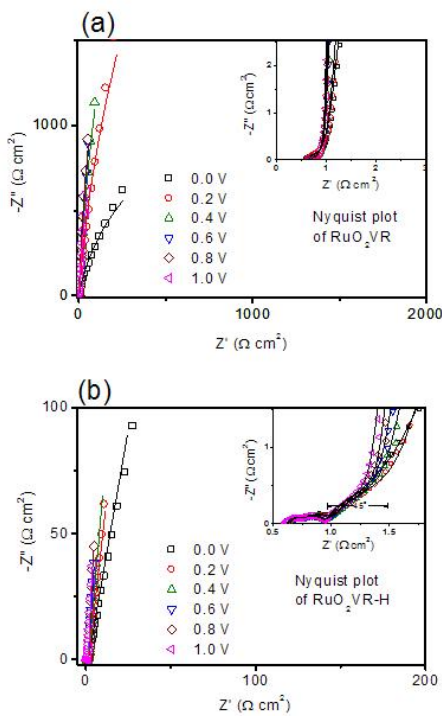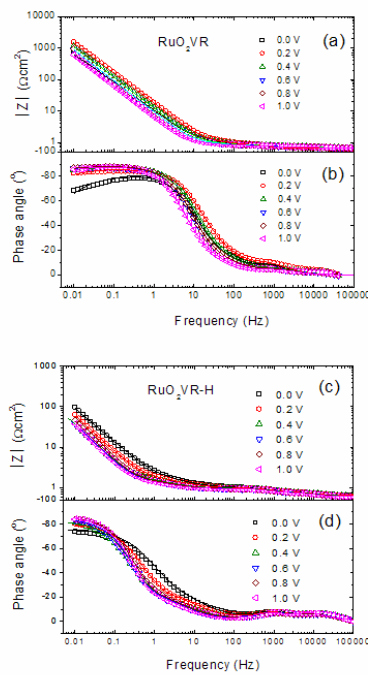Fig. 3 Nyquist plots of (a) RuO$_2$VR, (b) RuO$_2$VR-H at various bias.

Fig. 4 Bode plots of (a) |Z| (b) phase angle of RuO$_2$VR versus frequency, (c) |Z| (d) phase angle of RuO$_2$VR-H.